

Modelling of a micro-channel heat sink for cooling of high-power laser diode arrays

PIOTR FURMAŃSKI*
KADHIM THUALFAQIR
PIOTR ŁAPKA

Institute of Heat Engineering, Warsaw University of Technology,
Nowowiejska 21/25, 00-665 Warszawa, Poland

Abstract Micro-channel heat sinks are used in a wide variety of applications, including microelectronic devices, computers and high-energy-laser mirrors. Due to the high power density that is encountered in these devices (the density of delivered electrical power up to a few kW/cm^2) they require efficient cooling as their temperatures must generally not exceed 100°C . In the paper a new design for micro-channel heat sink (MCHS) to be used for cooling laser diode arrays (LDA) is considered. It is made from copper and consisting of 37 micro-channels with length of 9.78 mm, width of $190\ \mu\text{m}$ and depth of $180\ \mu\text{m}$ with the deionized water as a cooling medium. Mathematical and numerical models of the proposed design of the heat sink were developed. A series of thermofluid numerical simulations were performed for various volumetric flow rates of the cooling medium, its inlet temperature and different thermal power released in the laser diode. The results show that the LDA temperature could be decreased from 14 to 17% in comparison with earlier proposed design of the heat sink with the further drop in temperature obtained by applying indium instead of gallium arsenide as the soldering material between the LDA and MCHS interface. Moreover, it was found that the maximum temperature, and therefore the thermal resistance of the considered heat sink, could be decreased by increasing the coolant flow rate.

Keywords: Microheat sink; Laser diode arrays cooling; Numerical simulation

*Corresponding Author. Email: pfurm@itc.pw.edu.pl

1 Introduction

Small dimension of different devices and/or high heat dissipation problems have become a serious limitation in many industries (electronic industry, micro-chemical engineering, cooling of powerful laser mirrors, air conditioning, computers, etc.) [1,2]. Heat dissipation rates in devices based on the silicon integrated circuit (IC) technology, e.g., computer modules, has increased by several orders of magnitude and can reach levels that approach those encountered by space vehicles upon re-entry into the earth's atmosphere. High-energy-laser mirrors, surface-emitting laser diode arrays, and high-speed microelectronic devices can dissipate from 0.1 to 10 MW/m². However contrary to space vehicles the temperature rise must generally not exceed 100 °C. For example the highest heat dissipation achieved today reaches 0.4 MW/m² for a single chip computer module. The high-energy-laser mirrors typically absorb about 0.1% of incident laser energy which corresponds to heating rates from 0.1 to 1 MW/m². Despite of these high thermal loads the temperature variation of these mirrors must be minimal otherwise a distortion (as little as 250 Å) can seriously degrade their optical performance. Arrays of surface-emitting diode lasers, which are developed either as laser pumping sources and optical interconnects for the ICs or as two-dimensional communication-switching devices, require high capacity and high-efficiency heat sinks. Micro-channel heat exchangers (MCHE) offer solutions to thermal dissipation problems for many existing and developing applications.

The concept of the micro-channel heat exchanger was first presented by Tuckerman and Pease [3] and Swift *et al.* [4]. Two main types of MCHEs are usually considered: a micro-channel heat exchanger for heat exchange between hot and cold fluids and a micro-channel heat sink for heat exchange between a wall surface and fluid [5–7]. The MCHSs are typically composed of thin plates of metal (e.g., copper) or non-metal (e.g., silicon) of very small etched channels and fins in a parallel arrangement [8]. The MCHSs are manufactured using the same fabrication technique as electronic devices [3]. This technique permits manufacture of high precision channels with the channel widths or fin widths as small as 50 μm and channel heights of an order of several hundred microns [8,9]. The walls in the micro heat exchanger must have a thickness of the order of 100 μm to withstand the coolant pressure. In the MCHS heat source and a heat sink are brought into very close thermal proximity, thus minimizing the total thermal resistance. Heat conduction transfers heat from the operating device (heat

source) to the heat sink. Heat is then transferred from the heat sink to the surroundings by passing a coolant, usually a liquid (or nanoparticle liquid suspension), through the channels. A great amount of research was carried out to study influence of two-phase flows of the various cooling fluids the micro- and mini-channels as a part of the thermosyphon loop for cooling computers [10], thermal resistance of the walls in a heat exchanger with rectangular mini-channels [11], impact of different factors including fluid properties on flow boiling and its onset as well as condensation on intensity of heat transfer and pressure drop in the mini-channels [12–15]. The MCHEs have many advantages in comparison to conventional heat exchangers: a high heat transfer coefficient with values that rival boiling heat transfer, large surface area to volume ratio, and low thermal resistance due to their small characteristic dimensions [16,17]. However when liquids, like water, are used as coolants flowing through their channels the pressures drops are of the order of 70 kPa.

Recently a prototype of a miniaturized micro-channel heat sink with glass micro-pipes was proposed for a particular purpose of cooling high-power diode laser arrays (LDA), see Fig. 1. This design was thoroughly studied both experimentally and numerically [18]. The maximum in-junction plane temperature was in the range 45–65 °C with the experimentally registered peak temperatures (hot spots) in the left part of the laser diode array (see Fig. 1) reaching 75–110 °C for the power density lying in the range of 2–3.8 MW/m² (and coolant flow rates of 54.97–87.86 mL/min).

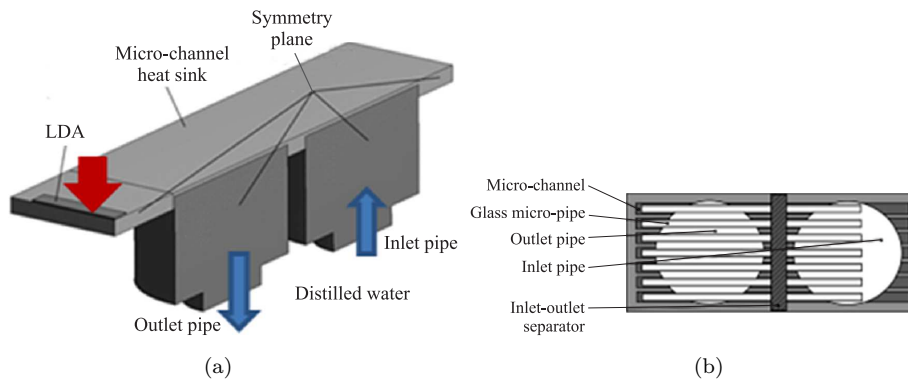


Figure 1: The old micro-channel heat sink design: (a) general view, (b) bottom part of micro-channel cooler [18].

The main objective of the current project was to propose a new design which could reduce the level of the maximum temperature closer to the required operation temperature 40–60°C and eliminate the hot spots while not changing the outer shape and coolant properties. Therefore, the external dimensions of the MCHS, LDA power density, coolant flow rates and inlet temperatures were kept the same as the previous design while the internal geometry of the heat sink was changed.

In the following sections of the paper the previous design of the MCHS was at first described in more detail and then the new design was proposed to enhance heat transfer in the heat exchanger and reduce its thermal resistance. Subsequently the mathematical and numerical models for heat transfer and fluid flow phenomena in this new design were presented. The final part of the paper is devoted to presentation of the simulation results, showing influence of the selected factors on the MCHS performance and its comparison with the previous design.

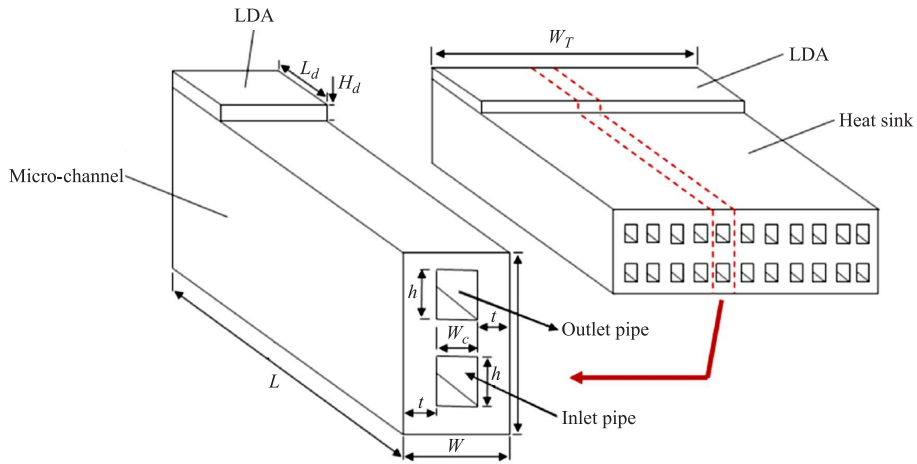


Figure 2: The heat sink geometry – proposed modifications in design

2 Description of the previous and new design of the micro-channel heat sink

The miniaturized micro-channel heat sink was proposed in [18] to cool a commercial laser diode arrays consisting of 66 individual emitters, Fig. 1a. As the laser resonator had the length of $L_d = 1$ mm, thickness of $H_d =$

100 μm and width of $W_T = 10$ mm therefore a compact design of the cooler was realized. The MCHS was made of copper with the length of $L = 5$ mm, width of $W_T = 10$ mm and height of 844 μm . Its body contained 14 micro-channels with the width of 370 μm and the depth of 410 μm . The glass micro-pipes which are placed in the channels had been blocked in the middle part of the cooler in order to separate the inlet and outlet pipes, Fig. 1b. The outer and inner diameters of micro-pipes were 320 μm and 200 μm , respectively. The laser diode array was soldered p-side down directly to the cover plate while the n-side electrical connections were attained by wire bonding [18]. The thermal contact resistance of joint between the LDA and the MCHS body was evaluated to be 0.5 K/W.

The deionized water was used as a cooling medium. The fluid entered the inlet port and flew through the micro-pipes into the region close to the laser diode array where it was heated. Subsequently, it was transported to the outlet port through gaps between walls of rectangular channels and the outer pipe surface, Fig. 1b.

The new design of the MCHS was also made of copper retaining the bulk dimensions of the heat exchanger. It consists of 37 micro-channels with the length of 9.78 mm and rectangular cross-section – the width of $W_c = 190$ μm and the depth of $h = 180$ μm – see Fig. 2. The separation walls have the thickness of $t = 80$ μm . The wall between the inlet part of micro-channel and the outlet part has the thickness of 180 μm . The thickness of the rear wall is assumed 200 μm . The deionized water enters each bottom channel and after reaching the region close to the laser diode array flows back through the upper channel, Fig. 3b.

3 Mathematical and numerical models of the microheat exchanger

Heat transfer in the MCHS occurs by heat conduction in the solid parts and heat convection in the fluid. Due to small dimensions of the channel heat conduction and viscosity in the coolant play the significant role [19–21]. The viscosity leads to increased energy dissipation and pressure drop in the heat sink [22,23]. The small lateral dimensions of the MCHS cause that the external heat losses can be treated as negligible. The flow in the micro-channels is usually laminar and incompressible however because of change in the direction of water flow close to the LDA, see Fig. 3b, the turbulent flow was assumed in the channels. The realizable k - ε turbulence

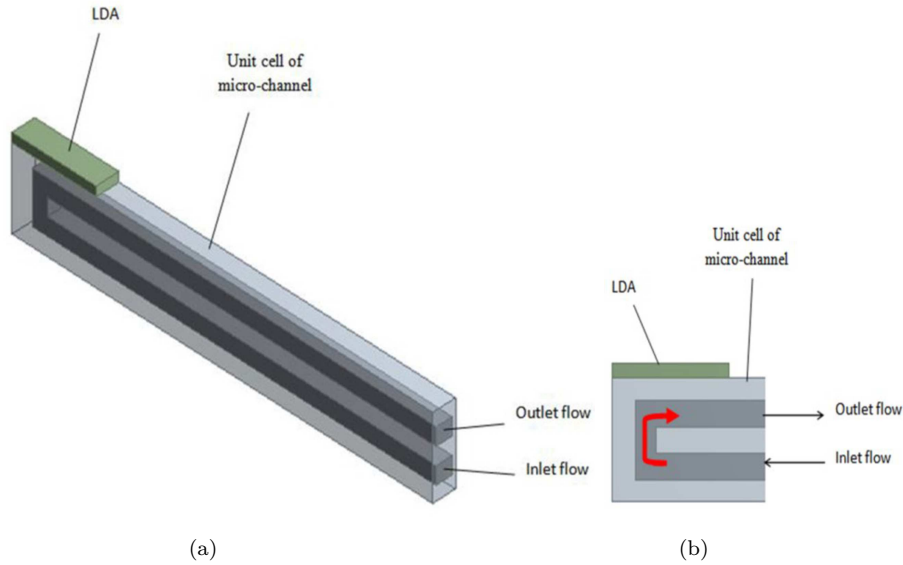


Figure 3: (a) Repetitive element of the microheat sink – LDA geometry and (b) flow direction in the proposed heat sink geometry.

model employing Boussinesq approximation was applied to find the turbulent viscosity with the default value of the turbulent Prandtl number [24]. Buoyancy effects in the fluid were neglected due to small transverse dimensions. Steady state of heat transfer and fluid flow and the constant thermophysical properties were assumed – see [18].

The heat was generated in the laser diode which was originally composed of InGaAlAs/GaAlAs/GaAs heterostructure, GaAs substrate and metal contacts. For simplicity the diode was assumed to be made from the gallium arsenide (GaAs) in a form of a thin slab with heat generation uniformly distributed in its volume. The thermal contact resistance of joint was represented by a thin layer of interface material between the LDA and the heat sink with the thickness derived from the thermal contact resistance evaluated in the original design. As the interface materials gallium arsenide and indium were used. The same thermophysical properties of materials as in [18] were adopted.

The inlet fluid velocity into the micro-channels and its temperature were uniform. At the exit the pressure outlet type of boundary condition was assumed. The upper and bottom external walls of the MCHS were convectively cooled being exposed to a surrounding (free convection) with

the ambient temperature 27°C and the convective heat transfer coefficient $5\text{ W/m}^2/\text{K}$. The lateral walls of the domain were assumed adiabatic. Due to assumed boundary conditions and symmetry of the geometry of the MCHS the computational domain of one micro-channel with a segment of the LDA was considered, see Fig. 3a.

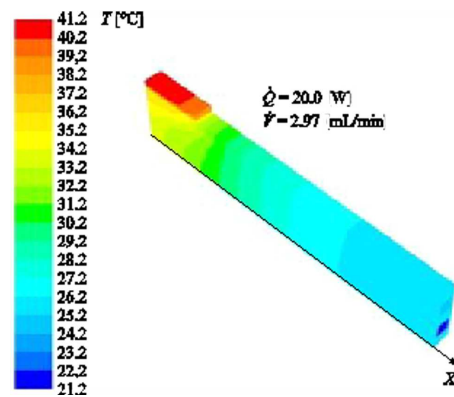


Figure 4: Temperatures distribution for the constant heat load $\dot{Q} = 20\text{ W}$ and volumetric flow rate of the cooling water $\dot{V} = 2.97\text{ mL/min}$.

The computational mesh consisted of approximately 700 000 hexahedral elements. The refined grid has been created in the flow zone, especially in the area under laser diode where the flow direction is changed. The turbulence model was supplemented with the respective wall treatment which required very fine mesh at walls with the first mesh node to be located at a distance no farther than the dimensionless distance $y^+ < 5$ from the wall.

The quality of the mesh was as follows: the aspect ratio varied from 1 to 34.8, the orthogonality from 0.28 to 1.0 and the skewness from 0.0 to 0.8. These parameters lie within the acceptable range. The grid convergence studies, i.e., influence of the mesh density on the obtained results were investigated. Two additional meshes finer (10% more elements as compared to the initial mesh) and coarser one (10% less elements as compared to the initial mesh) were generated. Then the temperature distribution on the surface of the LDA was found not to be significantly affected by the grid size, i.e., the relative mean absolute differences between temperature values on the surface of the LDA calculated applying different meshes were below 0.5%. The grid size had also minor effect on the pressure drop value. However, in this case the relative mean absolute differences between pressure drops calculated applying different meshes were higher than for tempera-

ture and were on the level of about 2% between the initial and coarse mesh and 1% between the initial and finer mesh. Therefore, accounting for accuracy of the pressure drop, the initial mesh was applied for the simulations.

The steady state calculations were performed using the finite volume method based commercial software ANSYS Fluent 15.0. In order to link the pressure and velocity fields the coupled scheme and pseudo transient formulation were used. The second order spatial discretization schemes were applied to all equations. The least squares cell based gradient reconstruction method was used to calculate gradients at the central nodes. The convergence criteria for all equations were set equal to 10^{-6} .

4 Results of numerical simulation

The influence of a few factors on the temperature distribution was analyzed, e.g., the heat load, volumetric flow rate and thermal contact resistance at the LDA–MCHS interface.

Distribution of temperature on the surface of the microcooler and laser diode for the heat load $\dot{Q} = 20$ W and volumetric flow rate of the coolant through one micro-channel $\dot{V} = 2.97$ mL/min is shown in Fig. 4. The highest temperature appears on the upper surface of the LDA and at the LDA-MCHS joint, see Fig. 5.

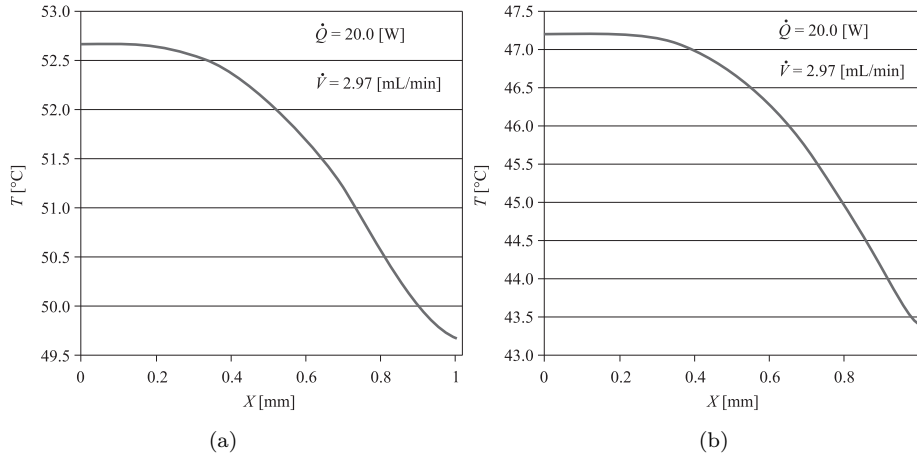


Figure 5: Temperature distribution along the symmetry plane of the computational domain: (a) on the upper surface of LDA, (b) at the junction.

Table 1: The results of numerical simulations.

Parameter	Case A-1	Case fA-2	Case A-3	Case B-1	fCase B-2	Case B-3	Case C-1	Case C-2	Case C-3
\dot{Q} ; W	20	20	20	29.7	29.7	29.7	38	38	38
\dot{V} [mL/min]	2.97	3.809	4.749	2.97	3.809	4.749	2.97	3.809	4.749
T_{in} ; °C	21.3	21.3	20.8	23.1	22.4	22	24.6	23.9	23.3
T_{max} ; °C at the surface of LDA	41.3	38.5	36.8	52.7	47.8	45.6	62.4	56.5	51.7
T_{max} ; °C at the junction	37.2	35	32.8	47.2	42.4	40.3	55.5	49.6	45
$T_{max} - T_{in}$; °C at the junction	15.9	13.7	12	24.1	20	18.3	30.9	25.7	21.7
Thermal resistance; K/W	0.795	0.685	0.6	0.81	0.673	0.616	0.813	0.676	0.571

Influence of three thermal loads (heat generated rates in the LDA): $\dot{Q} = 20$, 29.7, and 38 W and coolant volumetric flow rates: $\dot{V} = 2.97$, and 3.809, 4.749 mL/min were studied. The inlet temperatures were assumed in accordance with the values presented in [18]. The obtained results are presented in Tab. 1. Moreover the overall thermal resistance of the MCHS based on the difference between the maximum temperature at the joint and the coolant inlet temperature was calculated and shown in this table.

Subsequently the effect of varying value of the thermal contact resistance was investigated. Figure 6 presents temperature distribution on the upper surface of the LDA for dissipation power $\dot{Q} = 20$ W and $\dot{V} = 3.809$ mL/min for the lack of thermal contact resistance and thermal resistance of 0.13 K/W and 0.15 K/W corresponding to indium and gallium arsenide, respectively, as the binding material. The higher the contact resistance the higher temperature at junction was observed with no significant change in temperature variation along the LDA – heat sink junction.

Next the pressure drop along the MCHS channels was determined, see Fig. 7. It was found that the pressure drop attained from 6 to over 12 kPa in the considered range of the coolant flow rates. It almost linearly increased with the flow rate.

Finally, comparison with the results presented in [18] was carried out for the maximum temperature of the MCHS at its junction with LDA for the volumetric flow rate $\dot{V} = 2.97$ mL/min and three thermal loads, see Tab. 2.

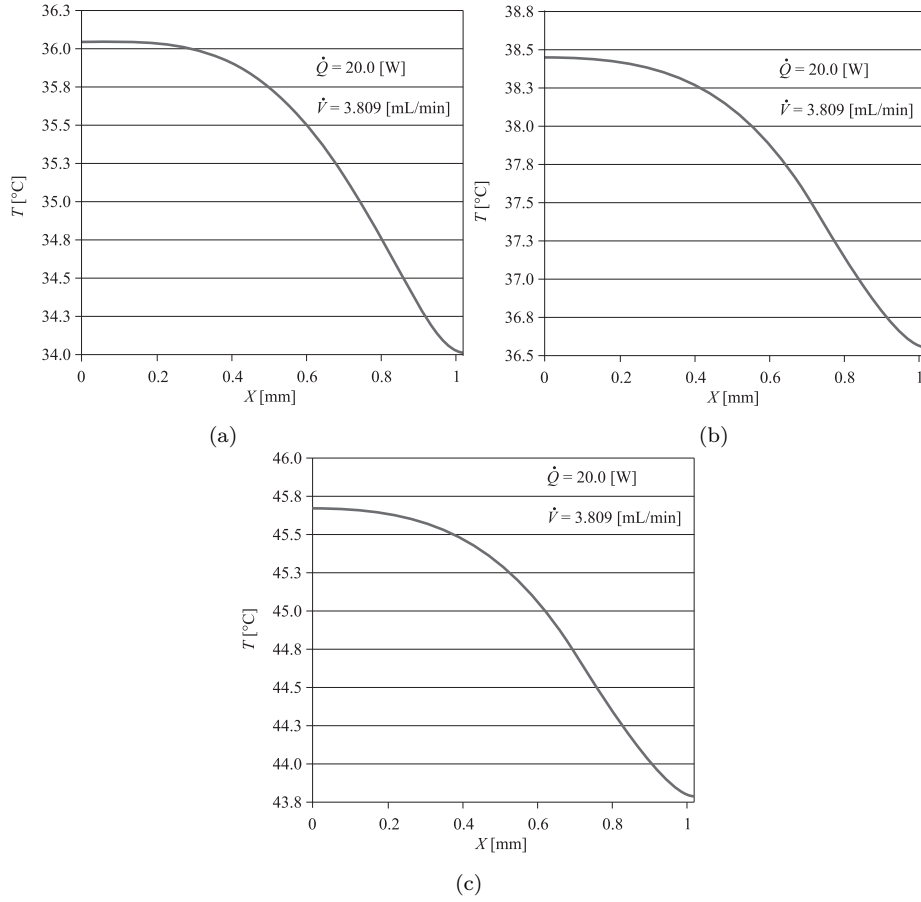


Figure 6: Temperature distribution along the symmetry plane of the computational domain on the lower surface of LDA for different binding materials: (a) lack of binding material – ideal contact, (b) indium, (c) gallium arsenide.

5 Conclusions

A design of the micro-channel heat sink is strictly related to its particular application. In the paper the MCHS was used for cooling the laser diode arrays (LDA). The LDA have small transverse dimensions and are usually located at the edge of the heat sink. The previous design of the MCHS recommended for the LDA cooling [18], which was studied both numerically and experimentally, was found unacceptable due to elevated temperature of

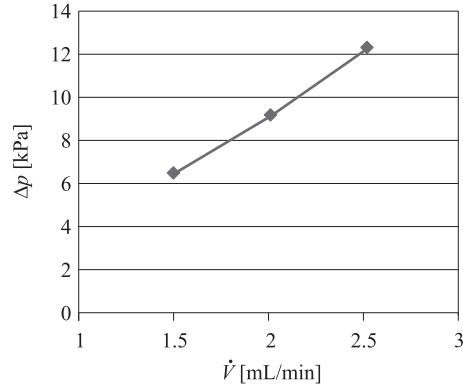


Figure 7: Pressure drop vs. flow rate for the copper and silicon MCHS.

Table 2: Temperatures [in °C] at junction between the microheat sink and the LDA.

Reference	Short description of micro-cooler design	Case A-1 $\dot{Q} = 20$ W	Case B-1 $\dot{Q} = 29.7$ W	Case C-1 $\dot{Q} = 38$ W
Original design [18]	Micro-pipes which transported cold fluid to heating section and located inside rectangular micro-channels (fluid outlets)	45	55	65
Proposed design	U-shaped micro-channel with inlet and outlet of the coolant. Change of the flow direction under the LDA	37.2	47.2	55.5

the LDA and appearance of the hot spots. Therefore a new design, which retains the external dimensions of earlier MCHS but differs by the coolant inlet and outlet forms as well by the shape, number and arrangement of the micro-channels, was proposed. As the first step of the design evaluation a numerical simulation was suggested and described in this paper. Analysis of influence of the heat generated in the diode, the volumetric flow rate of the coolant and thermal contact resistance between the LDA and the microheat sink on temperature distribution, thermal resistance and pressure drop of the coolant was accomplished. It was found that the new design leads to lower maximum temperature at the junction (by 10–15%) as compared to the original one. The maximum temperature on the up-

per surface of the LDA was established to be 3.5 to 6.9 °C higher than at the MCHS–LDA junction and depended on the thermal load applied to the micro-channel heat sink. It was also confirmed that the performance of the heat sink can be significantly improved and the observed hot spot eliminated by decreasing the thermal contact resistance at the LDA – heat sink junction plane and making it more uniformly distributed along the junction. The overall thermal resistance of the MCHS was considerably reduced by increasing the volumetric flow rate of coolant. The pressure drop in the coolant was found to be within the range observed for other MCHSs and almost linearly increased with the volumetric flow rate of the coolant.

Received 8 December 2017

References

- [1] ESCHER W., MICHEL B., POULIKAKOS D.: *A novel high performance, ultra thin heat sink for electronics*. Int. J. Heat . Fluid Fl. **31**(2010), 4, 586–598.
- [2] QU W., MUDAWAR I.: *Experimental and numerical study of pressure drop and heat transfer in a single-phase micro-channel heat sink*. Int. J. Heat Mass Tran. **45**(2002), 12, 2549–2565.
- [3] TUCKERMAN D.B., PEASE R.F.: *High performance heat sinking for VLSI*. IEEE Electron. Dev. Lett. EDL. **2**(1981), 126–129.
- [4] SWIFT G.W., MIGLIORI A., WHEATLEY J.C.: *Microchannel crossflow fluid heat exchanger and method for its fabrication*. U.S. Patent 4, 516, 632, May 14, 1985.
- [5] LI J., PETERSON G.P., CHENG P.: *Three-dimensional analysis of heat transfer in a micro-heat sink with single phase flow*. Int. J. Heat . Mass Tran. **47**(2004), 19, 4215–4231.
- [6] PELES Y. ET AL.: *Forced convective heat transfer across a pin fin micro heat sink*. Int. J. Heat Mass Tran. **48**(2005), 17, 3615–3627.
- [7] QU W., MUDAWAR I.: *Analysis of three-dimensional heat transfer in micro-channel heat sinks*. Int. J. Heat Mass Tran. **45**(2002), 3973–3985.
- [8] LI J., PETERSON G.P.: *3-Dimensional numerical optimization of silicon-based high performance parallel microchannel heat sink with liquid flow*. Int. J. Heat Mass Tran. **50**(2007), 15, 2895–2904.
- [9] MUNIR F.A. ET AL.: *The effect of parameter changes to the performance of a triangular shape interrupted microchannel heat sink*. J. Technol. (Sci. Eng.) **58**(2012), No. 2, 33–37.
- [10] BIELIŃSKI H., MIKIELEWICZ J.: *Computer cooling using a two phase minichannel thermosyphon loop heated from horizontal and vertical sides and cooled from vertical side*. Arch. Thermodyn. **31**(2010), 4, 51–59.

-
- [11] RYBIŃSKI W., MIKIELEWICZ J.: *Analytical 1D models of the wall thermal resistance of rectangular minichannels applied in heat exchangers*. Arch. Thermodyn. **37**(2016), 3, 63–78.
- [12] PIASECKA M.: *An investigation into the influence of different parameters on the onset of boiling in minichannels*. Arch. Thermodyn. **33**(2012), 4, 67–90.
- [13] MIKIELEWICZ D., JAKUBOWSKA B.: *Prediction of flow boiling heat transfer data for R134a, R600a and R290 in minichannels*. Arch. Thermodyn. **35**(2014), 4, 97–114.
- [14] MIKIELEWICZ D., ANDRZEJCZYK R., JAKUBOWSKA B., MIKIELEWICZ J.: *Comparative study of heat transfer and pressure drop during flow boiling and flow condensation in minichannels*. Arch. Thermodyn. **35**(2014), 3, 17–38.
- [15] SIKORA M., BOHDAL T.: *Modeling of pressure drop during refrigerant condensation in pipe minichannels*. Arch. Thermodyn. **38**(2017), 4, 15–28.
- [16] HARPOLE G.M., ENINGER J.E.: *Micro-channel heat exchanger optimization*. Semiconductor Thermal Measurement and Management Symposium, 1991. SEMI-THERM VII. Proceedings., Seventh Annual IEEE. IEEE, 1991.
- [17] UPADHYE H.R., KANDLIKAR S.G.: *Optimization of microchannel geometry for direct chip cooling using single phase heat transfer*. ASME 2004 2nd International Conference on Microchannels and Minichannels. American Society of Mechanical Engineers, 2004.
- [18] KOZŁOWSKA A. ET AL.: *Experimental study and numerical modeling of micro-channel cooler with micro-pipes for high-power diode laser arrays*. Appl. Therm. Eng. **91**(2015), 279–287.
- [19] HERWIG H.: *Flow and heat transfer in micro systems: Is everything different or just smaller?* ZAMM **82**(2002), 9, 579–586.
- [20] TAMMA K., ZHOU X.: *Macroscale and microscale thermal transport and thermo-mechanical interactions: some noteworthy perspectives*. J. Therm. Stresses **21**(1998), 3-4, 405–449.
- [21] ZHANG Z.M.: *Nano/Microscale Heat Transfer*. McGraw-Hill, 2009.
- [22] KALTEH M. ET AL.: *Experimental and numerical investigation of nanofluid forced convection inside a wide microchannel heat sink*. Appl. Therm. Eng. **36**(2012), 260–268.
- [23] KOO J., KLEINSTREUER C.: *Viscous dissipation effects in microtubes and microchannels*. Int. J. Heat. Mass Tran. **47**(2004), 14, 3159–3169.
- [24] VERSTEEG H.K., MALALASEKERA W.: *An Introduction to Computational Fluid Dynamics*, 2nd Edn., Pearson Education Ltd. 2007.